https://doi.org/10.2352/CIC.2025.33.1.32

Smartphone color quantification from a clinical perspective: accuracy and precision

Yifan Zhang, Terence S Leung, Department of Medical Physics and Biomedical Engineering, University College London, London, UK

Abstract

Smartphones, with their built-in cameras, are increasingly employed in clinical applications, e.g., screening patients for jaundice or anemia. In these applications, the color values of the target are converted into a biomarker using a regression or AI model. This paper investigated the accuracy and precision of x and y chromaticity values influenced by image noise and environmental factors, which could affect diagnostic performance. Accuracy was represented by the mean xy error distance (MED), and precision by the standard deviation (SD) of the xy chromaticity measurements. Using a Samsung S22 smartphone to take photos of the same color patch in 9 positions over 20°, we found that even for the same target, taking a photo from different angles caused the xy chromaticity values to change. However, the accuracy could be maintained by averaging these color measurements. The xy chromaticity measurements could also be affected by a neighboring color object and its impact on accuracy depended on the colors of the neighboring object and the target. We also investigated the scenarios with 3D graphics software Blender and found similar trends. Understanding factors influencing the accuracy and precision of color quantification can lead to improvements of smartphone imaging-based diagnostic techniques.

Introduction

Smartphones are increasingly employed in clinical applications. One application area is to use the smartphone camera to take photos of a patient and perform color analysis, resulting in important diagnostic information. For example, the "yellowness" of the skin or sclera of a newborn baby allows the identification of severely jaundiced babies due to the accumulation of the yellow-colored bilirubin in the blood turning skin tone yellow [1-3]. Another example is to identify anemic patients based on the paleness (or redness) of the patient [4]. Anemic patients, due to the lack of red blood cells in their blood, tend to have pale skin tone, most noticeable in regions with no or very little skin pigment (melanin), e.g., lower eye lid and lower lip/gum. The smartphone approach offers a point-of-care, low-cost screening technique for jaundice and anemia, reducing the number of invasive and costly blood tests.

While a diagnostic device requires robust, consistent readings, the color values, i.e., RGB or xy chromaticity values, captured by a digital camera are subject to variability due to image noise and environmental factors. The aims of this paper were to investigate the accuracy and precision of color quantification in a smartphone camera using controlled experiments and computer simulation with 3D graphics software Blender.

Methods

Metrics for quantifying accuracy and precision

In this work, we use the xy chromaticity as the color space since it is universal, allowing color measurements captured by different devices to be compared. In comparison to the L*a*b* color space, xy chromaticity has the crucial advantage that it is luminance-independent, meaning that color quantification is not affected by the magnitude of the illumination, which is important in a scientific measurement. The conversion from the native RGB space to the xy chromaticity will be discussed in the next section.

In this work, accuracy is measured (inversely) by the mean xy error distance (MED), i.e., the larger the MED, the lower the accuracy.

$$MED = \frac{1}{n}\sum_{i=1}^{n}\Delta xy_i \quad (1)$$

$$\Delta xy_i = \sqrt{(x_i - x_0)^2 + (y_i - y_0)^2} \quad (2)$$

x_0 and y_0 are the ground truth x and y chromaticity values as measured by a spectrophotometer; x_i and y_i are i^{th} x and y chromaticity values as measured by smartphone camera; n is the number of measurements.

Precision is measured (inversely) by the standard deviation (σ) defined as follows:

$$D_{xy}(i) = \sqrt{{x_i}^2 + {y_i}^2} \quad (3)$$

$$\overline{D_{xy}} = \frac{1}{n}\sum_{i=1}^{n} D_{xy}(i) \quad (4)$$

$$\sigma_{xy} = \sqrt{\frac{1}{n}\sum_{i=1}^{n}\left[D_{xy}(i) - \overline{D_{xy}}\right]^2} \quad (5)$$

Experiments

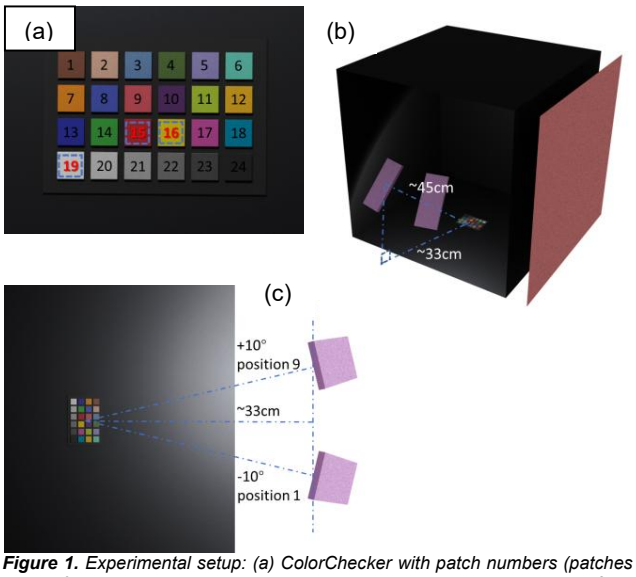

Figure 1. *Experimental setup: (a) ColorChecker with patch numbers (patches 15, 16 & 19 investigated here); (b) a smartphone (purple) takes photos of the ColorChecker at 9 different, equidistance positions between -10° and 10° in a shielded black environment with a neighboring wall with either pink (shown here) or black color; (c) top view*

Experimental setup

The entire experimental setup was constructed on a black, light-absorbing optical platform. A black curtain made of light absorbing material was draped over a rectangular frame to form an enclosed space measuring 60 cm × 50 cm × 60 cm (width × depth × height). As shown in Figure 1(a), a ColorChecker (Passport 2, Calibrite), was used as the target. We focused on three color patches of the ColorChecker in the following investigations, including the red (patch 15) and yellow patches (patch 16), relevant to anemia and jaundice screening, as well as the white patch (patch 19). The xy chromaticity values of the three color patches were measured by a spectrophotometer (ColorMunki, X-Rite) and used as the ground truth. The ColorChecker was positioned at the center of the optical platform.

A Samsung Galaxy S22 smartphone was mounted on a tripod, which could move in parallel to the optical platform. The tripod was equipped with angular markings to allow controlled adjustment of the smartphone's rotation angle. Figure 1(b) shows the Blender-rendered schematic of the experimental setup. The wall on the right was replaceable and the smartphone remains outside the box, movable in parallel to the optical platform.

Image capture with the smartphone

All images in this study were captured using an in-house app, which supports continuous capturing of raw .DNG images using predefined fixed settings: ISO 400, 1/20 s exposure time, and aperture at f/1.8.

Illumination during image capture was provided exclusively by the smartphone's built-in LED in torch mode. To eliminate any tripod vibrations caused by manual smartphone interaction, a 5-second delay was introduced after a button had been pressed to start the capture. Additionally, each measurement consisted of five consecutive captures to estimate the intrinsic variance of the smartphone camera.

Image processing and color space

The captured images were processed using Matlab 2023b. Regions of interest (ROIs) corresponding to the color patches on the ColorChecker were identified using a region-growing algorithm [5]. Both the threshold values and the initial seed pixels within each patch were manually adjusted to ensure accurate segmentation of the largest homogeneous region. The final RGB measurement for each patch was computed as the median value within the extracted region.

To ensure a consistent color representation and enable comparison with Blender simulation results, all color measurements were mapped to the CIE XYZ (D65) color space [6]. This space serves as a reference color space capable of integrating measurements across different devices. Furthermore, due to its linearity, despite slight perceptual deviations, it is well-suited for computational tasks in medical imaging. To eliminate the influence of luminance information, the final color measurement results used for comparison were expressed in terms of xy chromaticity. The xy chromaticity values were obtained based on the XYZ values using the following definitions:

$$x = \frac{X}{X+Y+Z}, \quad y = \frac{Y}{X+Y+Z} \tag{6}$$

The transformation from camera raw RGB (under the built-in LED flash) to CIE XYZ (D65) was performed using a 3×3 mapping matrix M, obtained via a prior camera calibration [7-9]. The matrix M was estimated using the Alternating Least Squares (ALS) method, which iteratively solves for both the mapping matrix and the local luminance distribution over the color checker patches in the calibration images [10]. The transformation from the camera local color space to the CIE XYZ (D65) color space was performed using the following equation:

$$\begin{bmatrix} X \\ Y \\ Z \end{bmatrix}_{D_{65}} = M \begin{bmatrix} R \\ G \\ B \end{bmatrix}_{camera} \tag{7}$$

Color quantification at different angles

As shown in Figure 1(b), when the smartphone was positioned at the midpoint along the edge of the platform, the distance between the smartphone camera and the target center was approximately 45 cm, while the tripod's base was approximately 33 cm away from the target center. This position served as the central reference point. While the smartphone might be moved laterally during the experiment, the height remained at a constant level.

Each movement step involved moving the tripod laterally, followed by rotating the smartphone towards the target either clockwise or counterclockwise by 2.5°, such that the target was once again centered in the smartphone's capture preview. Using this approach, the smartphone captured images from nine distinct positions arranged along a straight horizontal path—four to the left and four to the right of the central position—with each adjacent position spaced 2.5° apart.

These nine positions were labeled from 1 to 9, corresponding to -10°, -7.5°, -5°, -2.5°, 0°, 2.5°, 5°, 7.5°, 10° relative to the central axis, as illustrated in Figure 1(c).

Color quantification with a pink neighboring wall

In this experiment, the right-side of the box was replaced with a pink-colored panel measuring 60 cm × 50 cm, precisely covering the original wall area. For clarity in distinguishing between the two experimental conditions, the environment without the pink background panel is referred to as the black background, while the environment with the panel is referred to as the pink wall.

The image acquisition procedure in this section was identical to that described in the previous section.

Simulations with Blender

In this study, the entire experimental process was simulated using a rendering pipeline implemented in Blender (v4.3.2) with the LuxCoreRender (v2.10.0) engine [11]. The rendering was performed using a path tracing algorithm under an RGB-based rendering model.

Renderer settings

The renderer employed path tracing for image generation, with the maximum light bounce set to 24 and the minimum number of samples before rendering completion set to 600, in order to effectively control image noise. Multi-bounce was enabled for materials to ensure accurate simulation of indirect illumination. The color space was configured as Linear XYZ-D65 to produce linear color outputs suitable for analysis. The camera position and viewing angles in the simulations were configured based on the specific values described in the experimental setup section. The light source was modeled as a 5 mm × 5 mm square area light with an emission angle of 120°, designed to approximate the smartphone's built-in LED flash. The light source was assigned a white color with RGB values of [1, 1, 1].

To simulate the scenario in which the flash moves together with the camera, the light source was co-located with the camera position in all rendering scenes. Since this study primarily focuses on

chromaticity, the radiant flux and brightness of the light source can be arbitrarily set, as long as the rendered image pixels remain unsaturated and free from distortion. In this experiment, the light source was configured with an emission power of 0.3 and an efficiency of 15, which are commonly used settings for simulating LED light sources.

In the simulation, the "camera" was modeled as an ideal pinhole camera. The rendered images were therefore free from lens distortion, and the depth of field was infinite. The camera model itself was based on an RGB trichromatic response, without any spectral parameterization. The focal length was set to 25 mm, which only affected the equivalent field of view but had no impact on either depth of field or light throughput.

The rendered outputs were saved as .PNG images at a resolution of 1080p (1920 × 1080 pixels). These images were subsequently processed and analyzed using MATLAB.

Simulating the ColorChecker

The patches on the ColorChecker were coated with a specialized matte material, exhibiting approximately isotropic diffuse reflectance. Experimental observations also confirmed that specular reflection from these patches was minimal. Therefore, in the simulation, the patches were modeled as matte materials, which account only for diffuse reflection while ignoring any specular components [12, 13].

The specific color settings were derived from spectrophotometer measurements, ensuring accurate spectral representation. The color checker was modeled at the correct scale, and non-patch elements such as white grid lines and logos were omitted from the simulations.

Simulating the background

Both the black light-absorbing background material and the pink wall were selected to minimize specular reflection although they could not be completely eliminated. Therefore, in the simulations, these materials were modeled using a glossy material, with separately defined diffuse and specular reflectance properties.

The diffuse color was assigned based on spectrophotometer measurements, while the roughness parameter was set to 0.5—a commonly used value for low-gloss surfaces and fibrous materials [12, 13].

Experimental observations revealed that removing one black wall from the environment resulted in an average brightness reduction of approximately 4.6% across all color checker patches, indicating the non-negligible role of specular reflection from the background material. Accordingly, the simulations varied the specular intensity settings of the black wall to match the experimental conditions. The best fit was found with a specular color setting of approximately [0.25, 0.25, 0.25] (in XYZ), indicating that the surface reflects about 25% of the incident light.

Using the same methodology, the specular reflection of the pink wall was estimated to be approximately [0.19, 0.15, 0.16] (in XYZ).

Results

Color measurements: xy chromaticity

Figure 2(a) shows the part of the xy chromaticity diagram with three clusters corresponding to color measurements of the red (patch 15), yellow (patch 16) and white patches (patch 19). The ground truth is represented by asterisk *.

For each smartphone position, 5 measurements were taken although only 4 markers are visible in Figure 2(a) due to certain measurements overlapping with each other.

Figure 2(b) depicts four clusters of the xy chromaticity values of the yellow patch, corresponding to four different measurement conditions. With a black background, the ground truth was closer to the xy chromaticity measured at position 9 (a cluster of bold circles) than to the those measured at position 3 (a cluster of thin circles). With a pink neighboring wall, the cluster (crosses) shifted towards the red region (bottom right corner) of the xy chromaticity diagram. The ground truth in this case was closer to the xy chromaticity measured at position 3 (a cluster of thin crosses) than to the those measured at position 9 (a cluster of bold crosses).

The influence of the pink wall on color measurements of the red and white patches was similar, i.e., they shifted towards the red region of the xy chromaticity diagram (bottom right corner). As shown in Figure 2(c) after the shift, the xy chromaticity measurements captured in the presence of the pink neighboring wall (crosses) were in fact slightly closer to the ground truth than those without (circles).

Figure 2(d) again shows that the ground truth was in the middle of xy chromaticity measurements with a black background (crosses). The presence of the pink wall again shifted the cluster (circles, without the pink wall) to the bottom right (crosses, with the pink wall), making the cluster further away from the ground truth.

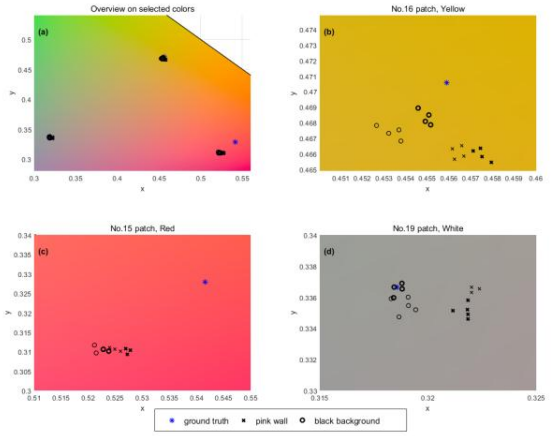

Figure 2. *The color measurements plotted on the CIE 1931 xy chromaticity diagram: (a) selected region showing xy chromaticity measurements of the red, yellow and white patches, (b) close-up of the yellow patch (no.16), (c) close-up of the red patch (no.15), (b) close-up of the white patch (no.19). Black background: thin circles correspond to the smartphone camera at position 3 (-5°); bold circles correspond to the smartphone camera at position 9 (+10°). Pink background: thin crosses correspond to the smartphone camera at position 3 (-5°); bold crosses correspond to the smartphone camera at position 9 (+10°); ground truth (measured by a spectrophotometer) represented by asterisk *.*

Smartphone at a fixed position

Tables 1 shows the accuracy (MED) and precision (SD) of 5 repeated measurements of xy chromaticity conducted by the smartphone at position 5 (0° in Figure 1). While the smartphone measurements of both the yellow and white patches had MED below 3.80, the MED for the red patch is higher at 23.79. The lower accuracy could be attributed to errors introduced by the calibration, which converted the native RGB space into the xy chromaticity space.

When a neighboring pink wall was introduced, the accuracies for measuring the yellow and white patches decreased (MEDs

increase) and their SDs increased. The accuracy for the red patch, on the other hand, increased slightly (MED decreases) because the shifted towards the red region of the xy chromaticity diagram is in the opposite direction of the calibration error, partially compensating for and reducing the overall error. The SD was also decreased by half.

Smartphone at variable positions

Tables 2 shows the accuracy and SD of color measurements conducted by the smartphone at 9 positions, i.e., -10°, -7.5°, -5°, -2.5°, 0°, 2.5°, 5°, 7.5°, 10° as defined in Figure 1. As 5 repeated measurements were taken for each position, there were a total of 45 measurements (n=45). As shown in Figure 2(b), four clusters appeared on the xy chromaticity diagram, depending on the position of the camera and the background color. Despite the differences in the color measurements for the same color patch, the accuracies (MED) for all the color measurements, calculated as averaged values, were similar to those in Table 1. The SDs in Table 2 were larger for the red and white patches, but smaller for the yellow patch. The results showed that averaging xy chromaticity measurements taken over a range of angles provided a similar accuracy to those taken at the same position.

Table 1 Accuracy (MED) and precision (SD) of 5 repeated color measurements with the camera at position 5 (n = 5)

Experiment	**Mean xy Error Distance [Standard Deviation] (×10^{-3})**		
Background Wall Color	Patch 15 (Red)	Patch 16 (Yellow)	Patch 19 (White)
All Black	23.79 [0.93]	3.78 [0.63]	0.92 [0.27]
1 Neighboring Pink Wall	22.34 [0.43]	5.37 [0.87]	4.35 [0.41]

Table 2 Accuracy (MED) and precision (SD) of 5 repeated color measurements with the camera at 9 different positions (n = 5×9 = 45)

Experiment	**Mean xy Error Distance [Standard Deviation] (×10^{-3})**		
Background Wall Color	Patch 15 (Red)	Patch 16 (Yellow)	Patch 19 (White)
All Black	24.77 [1.11]	3.78 [0.57]	0.79 [0.39]
1 Neighboring Pink Wall	23.19 [1.41]	5.27 [0.78]	3.70 [0.68]

Simulations

Figures 3(a)-(d) follow the same arrangement as Figure 2, and the simulated xy chromaticity measurements also have similar behavior as their experimental counterpart. For example, in the presence of a neighboring pink wall, the simulated xy chromaticity measurements also shifted towards the red region of the xy chromaticity diagram (bottom right corner).

In comparison to the experimental results in Figure 2, the simulated xy chromaticity measurements were closer to the ground truth for the red patch (see Figure 3(c)), and at similar distances for the yellow and white patches (see Figures 3(b) and 3(d)). This is consistent with the higher accuracies for measuring the red patch and the similar accuracies for the yellow and white patches, as shown in Tables 3 and 4.

In comparison to the experimental results in Figure 2, the scattering of simulated xy chromaticity measurements shown in Figure 3 was more confined. This is confirmed by the smaller SD in Tables 3 and 4. Image noise due to the electronics was not simulated, leading to a generally lower variability than the experimental results.

The fact that the simulated results were sufficiently close to the experimental results indicates that the factors considered in the simulations were representative of reality. These factors include specular reflectivity settings for the ColorChecker and the surrounding walls.

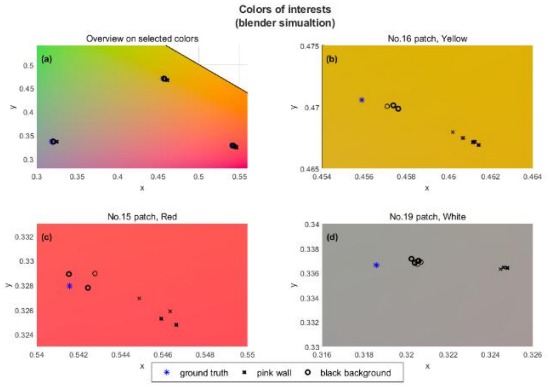

Figure 3. *Simulated color measurements plotted on the CIE 1931 xy chromaticity diagram: (a) selected region showing xy chromaticity measurements of the red, yellow and white patches, (b) close-up of the yellow patch (no.16), (c) close-up of the red patch (no.15), (b) close-up of the white patch (no.19). Black background: thin circles correspond to the smartphone camera at position 3 (-5°); bold circles correspond to the smartphone camera at position 9 (+10°). Pink background: thin crosses correspond to the smartphone camera at position 3 (-5°); bold crosses correspond to the smartphone camera at position 9 (+10°).*

Table 3 Accuracy (MED) and precision (SD) of 5 repeated simulated color measurements with the camera at the same position (n = 5)

Simulations	**Mean xy Error Distance [Standard Deviation] (×10^{-3})**		
Background Wall Color	Patch 15 (Red)	Patch 16 (Yellow)	Patch 19 (White)
All Black	0.83 [0.76]	1.73 [0.33]	1.86 [0.07]
1 Neighboring Pink Wall	4.56 [0.000]	5.75 [0.000]	5.99 [0.09]

Table 4 Accuracy (MED) and precision (SD) of 5 repeated simulated color measurements with the camera at 9 different positions (n = 5×9 = 45)

Simulations	Mean xy Error Distance [Standard Deviation] ($\times 10^{-3}$)		
Background Wall Color	Patch 15 (Red)	Patch 16 (Yellow)	Patch 19 (White)
All Black	1.23 [1.02]	1.56 [0.24]	1.90 [0.12]
1 Neighboring Pink Wall	5.23 [0.90]	5.74 [0.24]	6.05 [0.09]

Discussions

Color measurement experiments

The accuracies of all the experiments were reasonably high. However, this could be the result of averaging color measurements taken with a smartphone over a range of symmetrical angles, which in this case, means 9 measurements from -10° to 10°. Suppose the averaging is performed over only 5 measurements, from 0° to 10°, the averaged color measurement may have a lower accuracy.

In the experiment, the red patch had lower accuracies (large MEDs) than the other two patches (see Tables 1 and 2). This was due to the calibration error, i.e., error arising from the conversion of RGB to XYZ (equation 7), which could be reduced if an optimized calibration is performed.

As shown in Figure 2, the xy chromaticity measurements can be shifted towards the color region of a neighboring color object, which in this case towards the bottom right for the pink neighboring color. This is because the LED flash illuminates both the target and the neighboring object. Light reflected off the neighboring object has been “colored” by the object itself before reaching the target, altering its eventual color detected by the camera.

Only one single smartphone was used in this work. This study should be expanded to include and compare different types of smartphones in future studies.

Blender simulations

Due to the inherent limitations of Blender and LuxCoreRender, which operate under an RGB-based rendering model rather than a spectrally-based one, the simulated results could not yield physically precise outputs with high accuracy. Achieving such accuracy is particularly challenging given the small error scale involved in this study.

Nevertheless, the simulations still provided physically plausible and experimentally consistent, qualitative insights. The quantitative results were also generally within a comparable order of magnitude. More importantly, the simulations confirmed that color measurement results were highly sensitive to the material properties of surrounding objects. Even surface reflectance effects that were not visually obvious to human eyes could significantly influence the precision of color measurements required in medical imaging applications.

From another perspective, obtaining highly accurate, directionally dependent spectral reflectance profiles for real-world materials is extremely complex and time-consuming [14, 15]. This study circumvented that process by using a simplified simulation pipeline, achieving qualitatively correct and quantitatively relevant results with significantly shorter compute time. This demonstrates the practical advantages of using Blender-based rendering models for exploratory research.

It is acknowledged, however, that the simulation results remain constrained by the experimental setup. For future studies requiring higher precision, spectral reflectance measurement and spectrally-based rendering will be indispensable.

Conclusions

This paper investigated the accuracy and precision of color measurements using a smartphone camera. The xy chromaticity measurements can be influenced by the position of the camera. However, the accuracy can be maintained by averaging these color measurements. The xy chromaticity measurements can also be affected by a neighboring color object and its impact on accuracy depends on the colors of the neighboring object and the target. With careful consideration of assumptions, open-source 3D graphics software Blender can be employed to investigate these effects. Understanding factors influencing color measurements with a smartphone camera can potentially improve its application in clinical diagnosis.

Acknowledgements

This project is funded by the National Institute for Health and Care Research (NIHR) under its Invention for Innovation (i4i) Programme (Grant Reference Number NIHR205460). The views expressed are those of the author(s) and not necessarily those of the NIHR or the Department of Health and Social Care.

References

[1] F. Outlaw, M. Nixon, O. Odeyemi, L. W. MacDonald, J. Meek, and T. S. Leung, "Smartphone screening for neonatal jaundice via ambient-subtracted sclera chromaticity," *PloS one,* vol. 15, no. 3, p. e0216970, 2020.

[2] C. Enweronu-Laryea *et al.*, "Validating a Sclera-Based Smartphone Application for Screening Jaundiced Newborns in Ghana," *Pediatrics,* 2022.

[3] A. Mariakakis, M. A. Banks, L. Phillipi, L. Yu, J. Taylor, and S. N. Patel, "Biliscreen: smartphone-based scleral jaundice monitoring for liver and pancreatic disorders," *Proceedings of the ACM on Interactive, Mobile, Wearable and Ubiquitous Technologies,* vol. 1, no. 2, pp. 1-26, 2017.

[4] T. A. Wemyss *et al.*, "Diagnosing anaemia via smartphone colorimetry of the eye in a population of pregnant women," *Physiological Measurement,* vol. 13, no. 1, p. 01NT01, 2025.

[5] D.-J. Kroon. "Region Growing." https://www.mathworks.com/matlabcentral/fileexchange/19084-region-growing (accessed June 5.

[6] J. Schanda, *Colorimetry: understanding the CIE system*. John Wiley & Sons, 2007.

[7] M. Nixon, F. Outlaw, L. W. MacDonald, and T. S. Leung, "The importance of a device specific calibration for smartphone colorimetry," in *Color and Imaging Conference*, 2019, vol. 2019, no. 1: Society for Imaging Science and Technology, pp. 49-54.

[8] B. Funt, R. Ghaffari, and B. Bastani, "Optimal linear RGB-to-XYZ mapping for color display calibration," in *Color and Imaging Conference*, 2004, vol. 2004, no. 1: Society for Imaging Science and Technology, pp. 223-227.

[9] M. Nixon, F. Outlaw, and T. S. Leung, "Accurate device-independent colorimetric measurements using smartphones," *Plos one,* vol. 15, no. 3, p. e0230561, 2020.
[10] G. D. Finlayson, M. Mohammadzadeh Darrodi, and M. Mackiewicz, "The alternating least squares technique for nonuniform intensity color correction," *Color Research & Application,* vol. 40, no. 3, pp. 232-242, 2015.
[11] *LuxCoreRender*. (2025). [Online]. Available: https://luxcorerender.org/
[12] R. Montes and C. Ureña, "An overview of BRDF models," *University of Grenada, Technical Report LSI-2012-001,* 2012.
[13] D. Guarnera, G. C. Guarnera, A. Ghosh, C. Denk, and M. Glencross, "BRDF representation and acquisition," in *Computer graphics forum*, 2016, vol. 35, no. 2: Wiley Online Library, pp. 625-650.
[14] T.-Q. Han and H.-L. Shen, "Photometric stereo for general BRDFs via reflection sparsity modeling," *IEEE Transactions on Image Processing,* vol. 24, no. 12, pp. 4888-4903, 2015.
[15] A. Ngan, F. Durand, and W. Matusik, "Experimental Analysis of BRDF Models," *Rendering Techniques,* vol. 2005, no. 16th, p. 2, 2005.

Author Biography

Yifan Zhang obtained his BSc from Peking University (2016), MSc from the University of Chinese Academy of Sciences (2019), and PhD from University College London (2024). He is currently a Postdoctoral Research Associate in the Department of Medical Physics and Biomedical Engineering at UCL. His research interests lie in the clinical applications of smartphone imaging.

Terence S Leung received his BEng in Electromechanical Engineering and his PhD in Biomedical Signal Processing, both from University of Southampton (1994 & 1999). Since 2001, he has been working at University College London and is currently Professor of Digital Health in the Department of Medical Physics and Biomedical Engineering. His research interests include medical imaging, healthcare app development and physiological monitoring.